Journal of Modern Technology & Engineering
Vol.3, No.1, 2018, pp.143-154

MODELING THE DEFORMATION OF STABILIZED AND REINFORCED SUBGRADE SOIL

Saad Issa Sarsam[1]*, Ahmad Zuhair AL Sandok[1]

[1]Department of Civil Engineering, University of Baghdad, Baghdad, Iraq

Abstract. In this study, Asphalt stabilized soil and grid reinforced soil have been investigated. Specimens of 152mm diameter and 116 mm in height have been prepared, cured, and then tested under static loading. The load-penetration data were recorded for each case. Data were fed to the finite element software for the modeling process. An assessment was conducted to search for the best realistic simulation, therefore the finite element models were developed using ABAQUS 6.13 software package. For pure and asphalt stabilized soil, two different finite element models have been tried, an axisymmetric model and a three-dimensional (3D) model. On the other hand, the reinforcement layers were simulated with two deferent models, truss element and shell element, the analysis results were then compared with those of experimental tests. Perfectly plastic model has been adopted to simulate all of the reinforcement layers, i.e. geogrid, geosynthetic and geotextile. It was concluded that the finite element simulation has given a good agreement with that of experimental tests. The 3D and axisymmetric models has presented no significant difference in predicting a realistic deformation. When the reinforcement is included in the analysis, both of the shell and truss element as the reinforcement layer has shown a good agreement among them.

Keywords: *Asphalt, stabilization, deformation, modeling, finite element.*

Corresponding Author: *Professor Saad Issa Sarsam, Head of Department of Civil Engineering, University of Baghdad, Baghdad, Iraq, Phone: 00964-7901878167*
e-mail: saadisasarsam@coeng.uobaghdad.edu.iq

Received: *13 May 2018;* ***Accepted:*** *23 June 2018;* ***Published****: 02 August 2018*

1. Introduction

The behaviour of the granular soil subgrade reinforced by geogrid was investigated by (Sarsam & Al-Saidi, 2015). The main parameters that were adopted are geogrid type. The test results showed that 20% improvement of strength could be detected of sandy soil in presence of geogrid. The behaviour of grid reinforced granular material under the impact of repeated loading was studied by (Abu-Farsakh *et al*, 2011). The main parameters adopted are locations of geogrid, geometry, tensile modulus, and stress concentration. The experimental test results indicated that the inclusion of geosynthetic ensures a long lasting pavement structure by reducing excessive deformation and cracking as stated by (Anitha, 2017). The influence of geosynthetic as a reinforcement on the California bearing ratio of the soil with various types of geotextiles has been investigated by (Ullagaddi & Nagaraj, 2013). The outcome of tested specimens indicated that the addition of geosynthetic in form of geotextile and geogrid reduces pavement thickness significantly. Reinforced pavement by geogrid subjected to cyclic loading (plate load test) was explored by (Chen & Farsakh, 2012). The method of analysis adopted by the study was the Mechanistic-Empirical Pavement Design Guide. Based on the test results, it was concluded that the presence of geogrid increases the resilient modulus of the coarse base in the range (10-90%) and reduced the

thickness about (12-49%), also an improvement in performance of the coarse base was observed when high tensile modulus geogrid were implemented. The benefits of geogrid adopted as reinforcement have been discussed by (Archer & Wayne, 2012), the soil layers exhibit increased stiffness of pavement. The best decision for selection of the suitable type of geogrid were based on the behaviour and benefits demonstrated for a particular product or set of products in full-scale pavement test geometry. A radical change in performance of the geogrid that reinforced the unbound granular materials was examined by (Chen *et al.*, 2012), and evaluated. The repeated loading was applied on the reinforced and unreinforced unbound granular specimens. The results showed that there was reductions in deformation due to the presence of geogrid reinforcements. The interactions behaviour between soil and geogrid by pull out test was evaluated by (Giang *et al.*, 2010). The parameters adopted are types of geogrid, and the quality of sand surrounding the geogrid. The shear strain distribution due to repeated loading was obtained. (Sarsam *et al.*, 2014) Investigated the influence of reciprocal action between soil and reinforcement strips and considered there was a frictional force at the interface. The pull out test was adopted to test the specimens under cured conditions and the presence of MC-30 cutback asphalt for stabilization. The laboratory test included the specimen that represented reinforced embankment model box. The reinforcements selected in the study are plastic material and aluminium as strip form that reinforced the compacted layers inside the box. The strips were subjected to a pull out test to explore the frictional forces that developed between the interface of soil and strips. The test results showed that the shear stress increased as the period of curing increased and the use of cutback asphalt as stabilizer material gave a high pull out stress as compared with the soil without stabilizer. A three-dimensional Finite Element (FE) analysis was developed by (Abu-Farsakh *et al.*, 2018) to simulate the fully-instrumented geosynthetic reinforced soil, PLAXIS 3D was selected to simulate the GRS-IBS behaviour under different loading conditions. The soil-structure interaction was simulated using zero thickness interface elements, in which the interface shear strength is governed by Mohr-Coulomb failure criterion. The results showed that the Federal highway administration analytical method is 1.5–2.5 times higher than those predicted by the FE analysis, depending on the loading condition and reinforcement location.The performance of the Geosynthetic Reinforced Soil was evaluated by (Ardah *et al.*, 2018) in terms of reinforcement strain, lateral facing deformation, and lateral facing pressure. Four different differential settlement values of 50, 100, 150, and 200 mm were selected for the study under three different service loading conditions. Simulations were conducted using two-dimensional (2D) PLAXIS. The results of FE analyses indicate that the differential settlement under the reinforced soil has a high impact on both the strain distribution along the reinforcement and the lateral facing displacement.

In this investigation, Asphalt stabilized soil and grid reinforced soil are investigated. Specimens of 152 mm diameter and 116 mm in height will be prepared, cured, and then tested under static loading. The load-penetration data will be recorded for each case, fed to the finite element software for the modelling process. An assessment will be conducted to search for the best realistic simulation, therefore the finite element models were developed using ABAQUS 6.13 software package.

2. Materials and Methods

2.1. The subgrade Soil

The sub-grade soil was obtained from a depth of (1 to 2.5 m) after removal of the top soil. Grain Size distribution of this Soil was found by Sieve analysis. The results are shown in Fig.1. Soil is classified as (SM) by Unified Soil Classification System (USCS) according to (ASTM D 2487, 2009). Using American Association of State Highway and Transportation Officials (AASHTO, 2013), the subgrade soil was classified as (A-1b). Table 1 presents the physical and geotechnical properties of the soil.

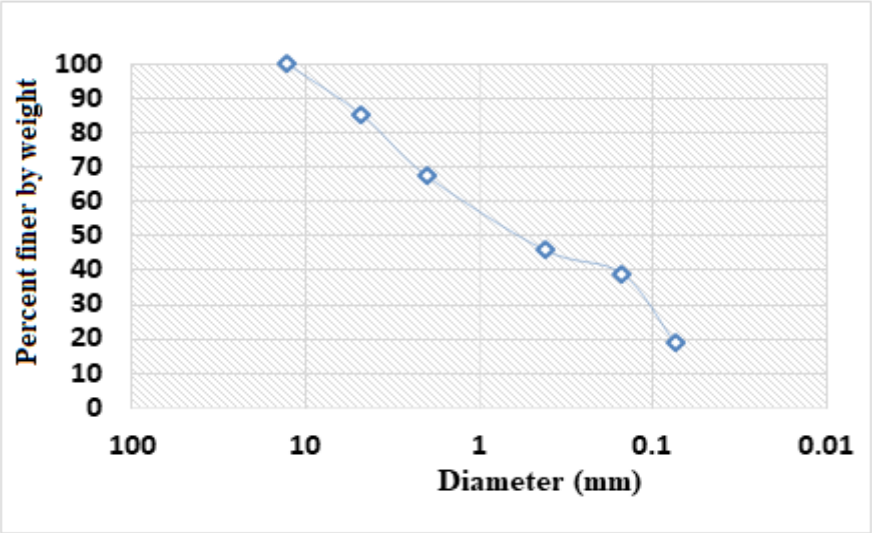

Figure 1. Grain size distribution of the soil

Table 1. Physical and geotechnical properties of the soil

Property	Test results
Percent passing 0.075 mm sieve	18.7
(AASHTO, 2013) Classification	A-1b
Unified soil classification	SM
Specific gravity	2.64
Liquid limit %	23
Plasticity index %	Non plastic
Maximum dry density (gm/cm^3) (Modified compaction)	1.76
Optimum water content %	16
Cohesion kPa (Direct shear box)	41
Angle of internal friction	29.2
Undrained shear strength kPa (Unconfined compression test)	50

2.2. Cutback Asphalt

Medium curing Cutback Asphalt (MC-30) was obtained from Dora refinery and implemented in this investigation. It is composed of 91.2% asphalt cement of grade 85-100, and 8.8% Kerosene. The Properties of Cutback Asphalt (MC-30) as supplied by the refinery are illustrated in Table 2. This grade of cutback gives low Viscosity and

has more solvent content which furnishes better mixing and coating of Soil′s Particles and better compaction.

Table 2. The properties of Cutback Asphalt (MC - 30) as supplied by Dora refinery

Property	Results
Flash Point (C.O.C) °C (min.).	38
Viscosity (C. st.) @ 60 °C.	30 – 60
Water % V (max.).	0.2
Distillation Test to 360 °C, Distillate % V of Total Distilled To 225 °C (max.). To 260 °C (max.). To 315 °C (max.).	 25 40 – 70 75 – 93
Residue from distillation to 360 °C % V (min).	50

2.3. Soil Reinforcements

2.3.1. Polypropylene Geogrid

Table 3 present the physical and mechanical properties of geogrid as supplied by the manufacturer.

Table 3. The Physical and Mechanical Properties of Polypropylene Geogrid

Property	Unit	Polypropylene Geogrid
Mass per unit area	g/m²	744
Rib thickness	mm	1.65×1.50
Junction thickness	mm	2.80
Tensile strength	MPa	9
Percentage elongation at maximumload	%	6

2.3.2. Glass Fibre Geosynthetic Mesh

This mesh is an alkali-resistant glass fabric. The properties as supplied by the manufacturer are presented in Table 4.

Table 4. Reinforcing Geosynthetic Mesh properties

Property	Value
Weight/unit area	160
Mesh size	4 x 4 mm
Initial tear strength	2200 N/5 cm
Rib thickness	0.5 mm
Ceiling area	4-5 minutes/m^2

2.3.3. Geotextile

Geotextile are permeable non-woven fabrics which, when used in association with soil, have the ability to separate, filter, reinforce, and protect. The three type of soil reinforcement are shown in Fig. 2.

Figure 2. Soil reinforcement implemented

2.4. Preparation and Testing of Specimens

The dry soil was mixed with optimum water content for two minutes to become homogenous, then it was mixed with the required percentage of cutback asphalt for three minutes so that the soil particles are coated with thin film of asphalt. The mixture was left for aeration at room temperature of 25°C for two hours before compaction. The procedure of obtaining the optimum percent of cutback asphalt, and obtaining the aeration and curing periods are published elsewhere, (Al Sandok, 2018). The mixture after aeration was then transferred into the mold and subjected to static compaction to a target density of 1.760 gm/ cm^3. Specimens were prepared with optimum fluid content (water +cutback asphalt) of 16%. Specimens were left for curing at room temperature of 25±2°C for seven days before testing. A total of 10 Stabilized soil specimens of 152 mm in diameter and 116 mm in height have been compacted to the target density using static compaction at a loading rate of 4 mm /min. until the required height was reached. The cured specimen was then subjected to the California bearing ratio test, and the load-penetration data were recorded. Fig. 3 shows the testing setup.

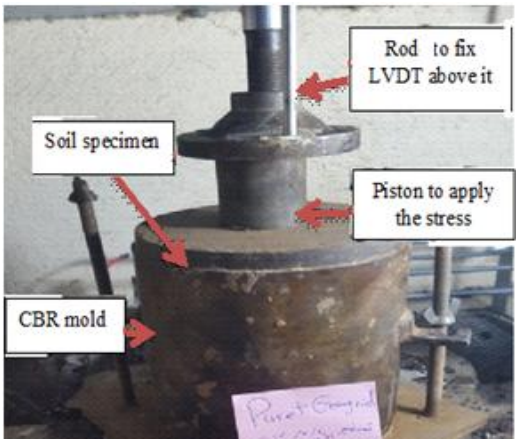

Figure 3. Testing setup

3. Results and discussion

Abaqus is an effective engineering software that adopt the finite element analysis to solve almost all stress analysis problems starting from relatively simple linear analysis up to the most difficult non-linear simulations. Abaqus has an exhaustive library of elements that can model practically any geometry. Abaqus library has an extensive list of materials models in which the behavior of the most engineering materials can be simulated.

3.1 Physical Properties

For pure and asphalt stabilized soil specimens, the cylinder model with radius of 75mm and height of 116.6mm was simulated using axisymmetric stress element and 3D stress element as show in Fig. 4. However, the adopted material properties were as indicated in Table 1.

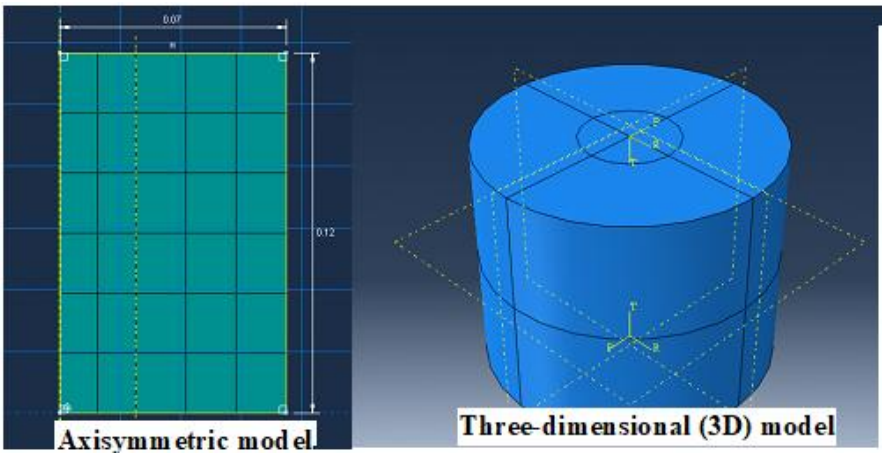

Figure 4. The axisymmetric and three dimensional models adopted

3.2. Choosing the Mesh Type and Size

ABAQUS CAX4R element has been adopted in the first model, which is a 4-node bilinear axisymmetric quadrilateral, reduced integration element. Where for the 3D model a C3D8R element has been adopted, which is an 8-node linear brick, reduced integration element. After performing multiple analysis with various mesh sizes an approximate mesh size of 15x19 mm was adopted for the axisymmetric model while an auto mesh was assigned for the 3D model to maintain compatibility as shown in Fig. 5.

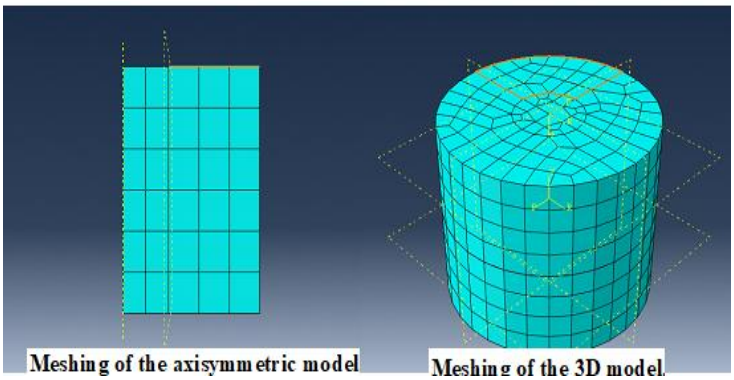

Figure 5. Mesh type and size

In the model with static load, a displacement control was adopted in the analysis by assigning 5mm displacement in the global (y-direction) at the center point, however to simulate the actual loading area, all points laying in that zone were attached to that center point. In the second model with the static load, also a displacement control was adopted in the analysis by assigning 5mm displacement in the global (y-direction) at the

center point, however to simulate the actual loading area, all points laying in that zone were attached to that center point. The movement in the radial direction was constrain for the perimeter, as it was constrained in the global (y-direction) for the model base as shown in Fig. 6.

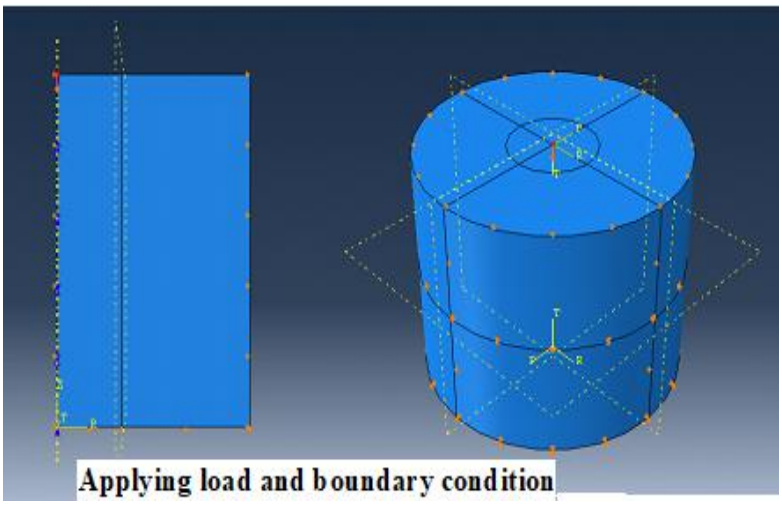

Figure 6. Load and boundary conditions

3.3. For the grid reinforced soil

An investigation was conducted for the best simulation, thus the reinforcement layers were simulated with two deferent models, truss element and shell element as shown in Fig.7, while Fig.8 exhibit the meshing of both elements.

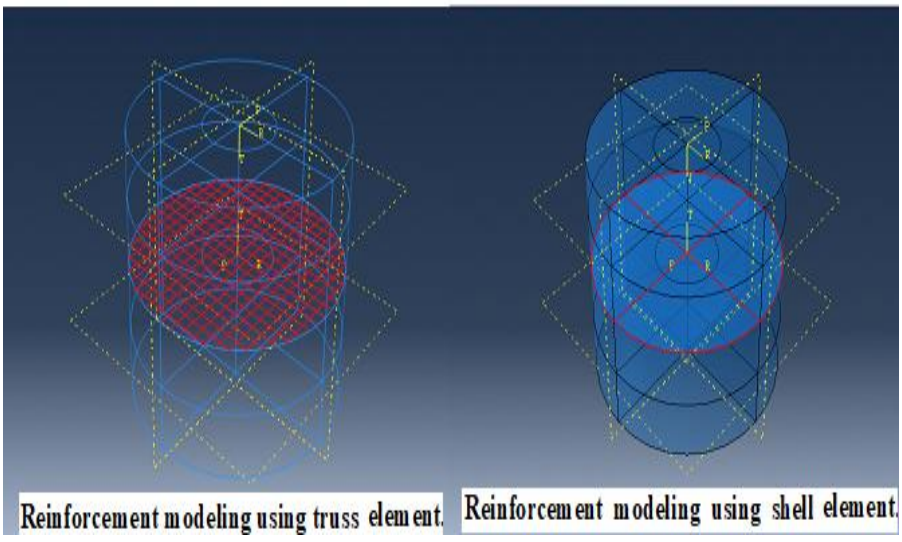

Figure7. Truss and shell elements

Abaqus assumes that contact between surfaces is frictionless. But it can include a friction model as part of a surface interaction definition, which has been adopted in this study by assigning the coefficient of friction of 0.5 between the soil-geogrid interfaces, i.e. The Coulomb friction model were adopted with a friction coefficient (μ=0.5).

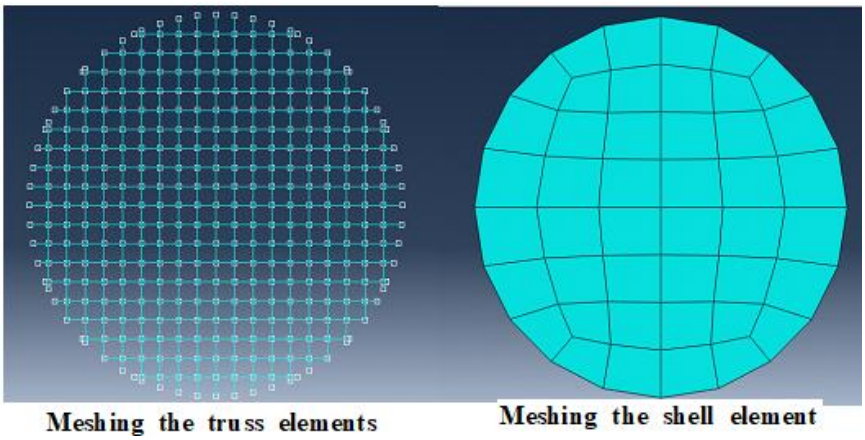

Figure 8. Meshing of the elements

3.4. Numerical Analysis with static load

3.4.1. for pure soil

Fig.9 represents the Mises stress and the deformation counter which has been pointed out for pure (natural) soil.Fig. 10 shows the load – deformation curve fore C.B.R specimens of pure soil for experimental and numerical with axisymmetric and 3D models.

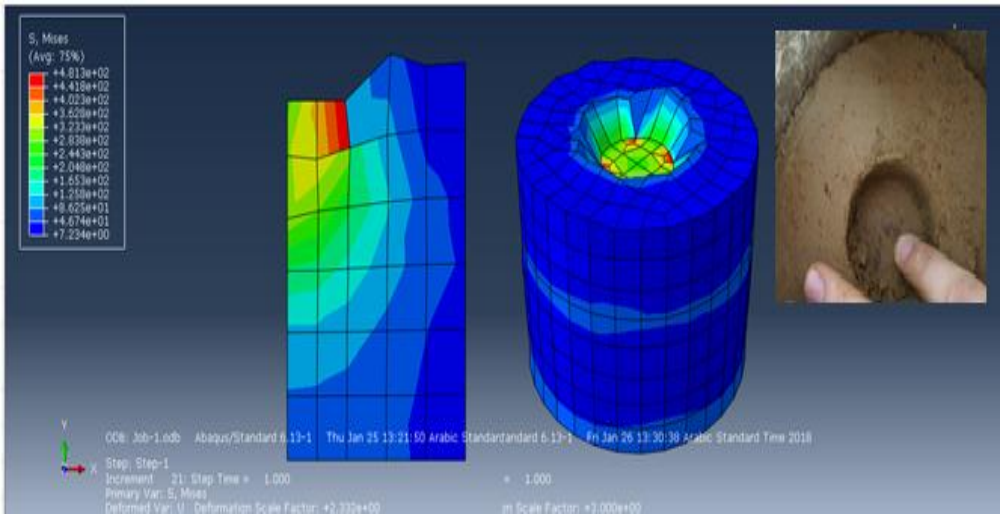

Figure 9. Mises stress and deformation counter for natural soil

It can be noticed that the curves from the axisymmetric and 3D model start as linear relation and the resistance to load increase with increasing the deformation until it reaches 2 mm, then the curve from 3D model exhibit concave down trend larger than the axisymmetric model. On the other hand, the experimental test exhibit sharp increase and better resistance to the loading up to 2mm deformation, then the trend goes linear. At failure, it can be observed that the experimental and axisymmetric models can sustain the load higher than the 3D model by (12 and 16) % respectively at 5 mm deformation. Such finding is in agreement with (Sarsam & Al-Saidi, 2015).

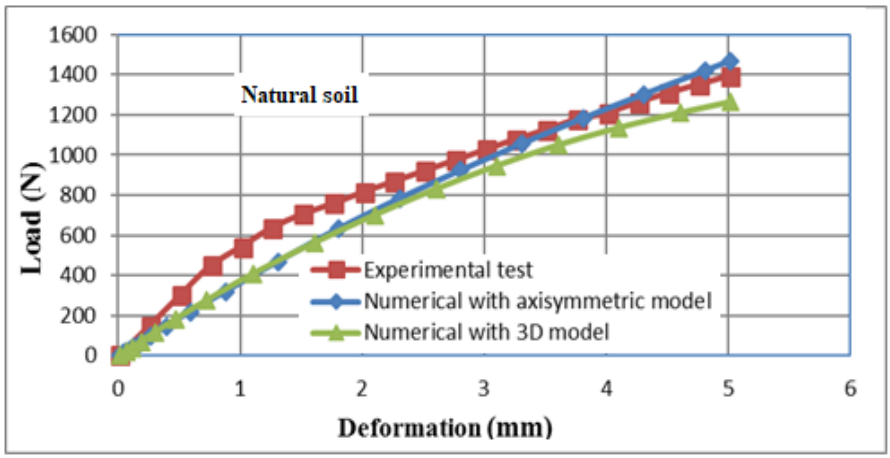

Figure 10. Load- deformation behavior for natural soil

3.4.2. For asphalt stabilized soil

Fig. 11 demonstrates the Mises stress and the deformation counter which has been pointed out for asphalt stabilized soil.Fig. 12 shows the load – deformation curve fore C.B.R specimens of asphalt stabilized soil for experimental and numerical with axisymmetric and 3D models. It can be noticed that these curves of the axisymmetric and 3D model start as linear relation and the resistance to load increase with increasing the deformation until failure at 5mm with no significant deference. The curve of experimental test exhibit concave down trend while the variation between 3D and axisymmetric models is not significant. The variation in load sustaining ability of the three models at failure (5mm deformation) is not significant. On the other hand, at 2mm deformation, the experimental test exhibit higher load resistance by 20% as compared to that of 3D and axisymmetric models. The ability of asphalt stabilized soil in resisting the deformation and sustaining the load is two folds higher than that for pure soil condition regardless of the modeling adopted. Load bearing phenomena of asphalt stabilized soil is in agreement with the work reported by (Sarsam & Ibrahim, 2008) and (Sarsam & Barakhas, 2015).

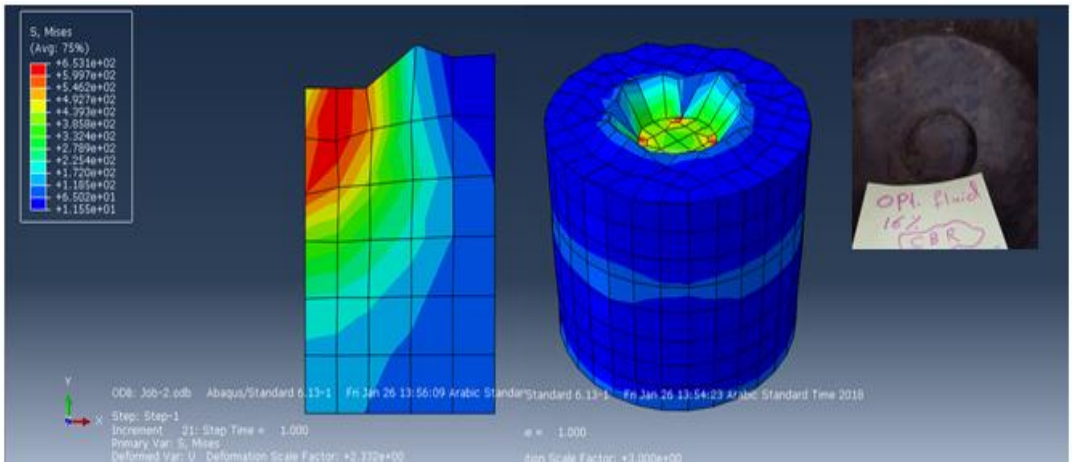

Figure 11. Mises stress and deformation counter for asphalt stabilized soil

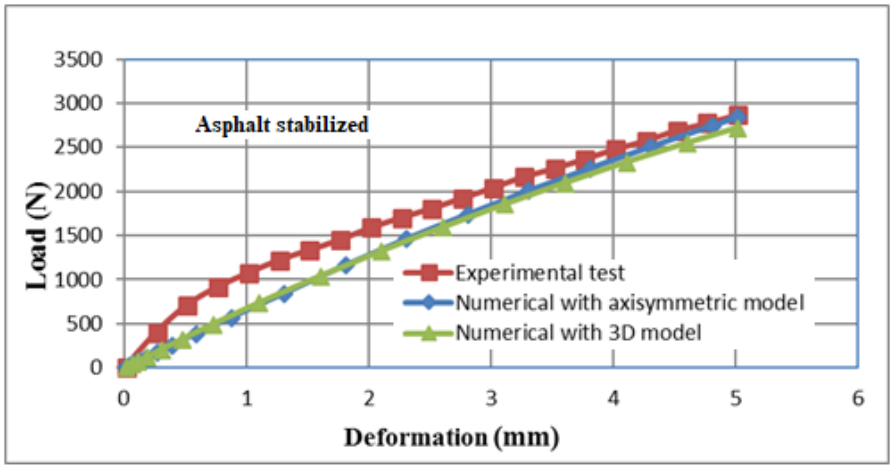

Figure 12. Load- deformation behavior for asphalt stabilized soil

3.4.3. Grid Reinforced Soil

Fig. 13 represents the deformation for the grid reinforced model with truss and shell element for reinforced subgrade soil. Fig. 14 exhibit the load – deformation curve fore C.B.R specimens of grid reinforced soil for experimental and numerical with axisymmetric and 3D models. It can be noticed that the curves from the axisymmetric and 3D model are almost linear and no significant variation could be observed in the behavior of both models. However, the experimental test start as linear relation and the resistance to load increase with increasing the deformation until it reaches 0.5mm deformation, after that the curve exhibit concave down trend and the load resistance increased as deformation increased until failure. The experimental test shows higher load resistance at failure by 10% as compared to that of numerical studies. Similar behavior was reported by (Sarsam & Al-Saidi, 2015) and (Sarsam & Al-Saeidy, 2014).The variation in load bearing behavior between asphalt stabilized and grid reinforced soil models is not significant.

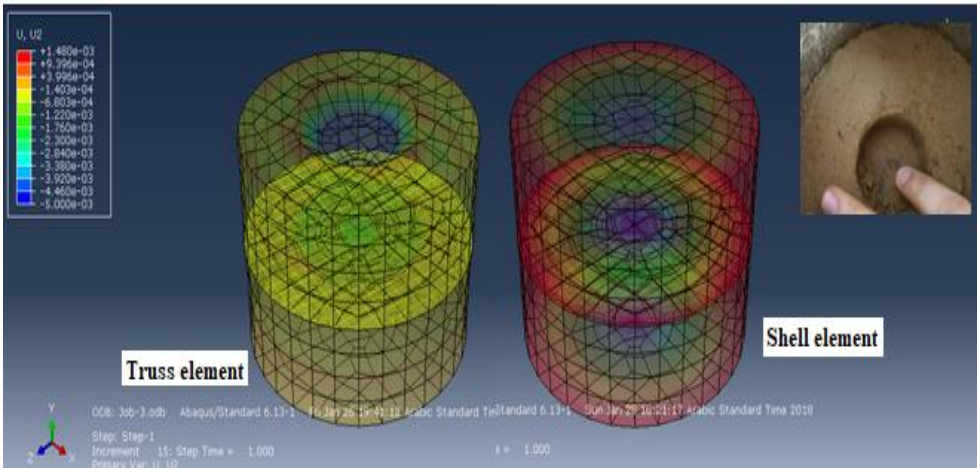

Figure 13. Mises stress for grid reinforced soil model

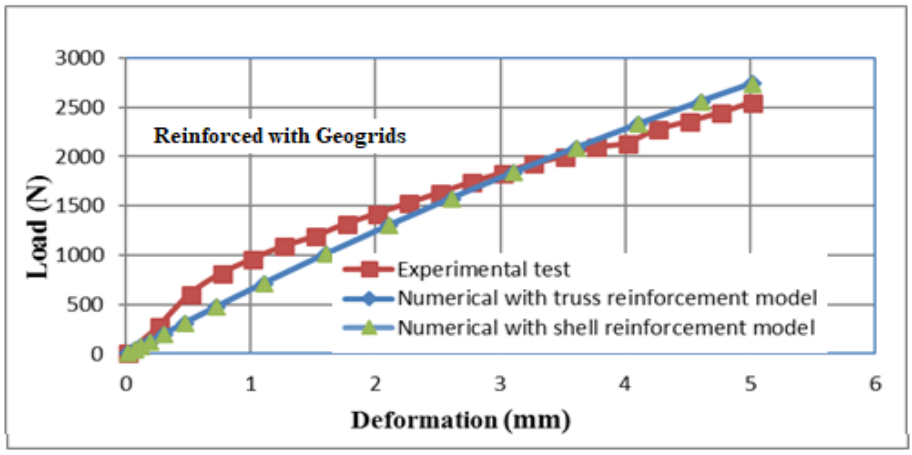

Figure 14. Load- deformation behavior for grid reinforced soil

Table 5 summarizes the deformation behavior of soil under CBR load for pure, stabilized and reinforced subgrade models. All these models shows the load in (KN) as dependent variable (y) and the deformation in mm as independent variable (x) at the top surface of the specimen under CBR test.

Table 5. Experimental and numerical modeling obtained

Specimen type	Experimental model	Numerical model
Natural (pure) soil	$y = -36.087x^2 + 431.67x + 86.813$ $R^2 = 0.9897$	$y = -28.543x^2 + 393.78x + 2.9694$ $R^2 = 0.999$
Asphalt stabilized soil	$y = -53.27x^2 + 779.24x + 234.91$ $R^2 = 0.9903$	$y = -30.216x^2 + 692.33x + 4.4958$ $R^2 = 0.999$
Soil reinforced with geogrid	$y = -54.547x^2 + 726.14x + 178.31$ $R^2 = 0.9897$	$y = -25.399x^2 + 671.98x + 2.7347$ $R^2 = 0.999$
Soil reinforced with geosynthetic	$y = -6.705x^2 + 239.22x + 27.869$ $R^2 = 0.9961$	$y = -27.273x^2 + 389.02x + 0.4124$ $R^2 = 0.999$
Soil reinforced with geotextile	$y = -29.619x^2 + 452.95x + 82.121$ $R^2 = 0.9933$	$y = -27.273x^2 + 389.02x + 0.4124$ $R^2 = 0.999$

4. Conclusion

Based on the testing program and finite element analysis, the following conclusions are drawn.

1. The finite element simulation has given a good agreement with that of experimental tests.
2. The experimental and axisymmetric models can sustain the load higher than the 3D model by (12 and 16) % respectively at 5 mm deformation.
3. The ability of asphalt stabilized soil in resisting the deformation and sustaining the load is two folds higher than that for pure soil condition regardless of the modeling adopted.
4. For asphalt stabilized soil at 2mm deformation, the experimental test exhibit higher load resistance by 20% as compared to that of 3D and axisymmetric models.
5. When the reinforcement is included in the analysis, using shell element as the reinforcement layer has shown a good agreement by comparing it with the truss

elements, the experimental test shows higher load resistance at failure by 10% as compared to that of numerical studies.

References

Sarsam S.I. & Al-Saidi, A. (2015). Impact of Plastic Grid Reinforcement on Behavior of Composite Soil Embankment Model. *Open Journal of Functional Material Research*, OJFMR, *2* (2).

Abu-Farsakh M., Souci, G., Voyiadjis, G.Z. & Chen, Q. (2011). Evaluation of factors affecting the performance of geogrid-reinforced granular base material using repeated load triaxial tests. *Journal of Materials in Civil Engineering*, *24*(1), 72-83.

Anitha J. (2017). Effect of geosynthetic on soft subgrade –literature review, *International Research Journal of Engineering and Technology* (IRJET), *4(*1), 1446-1448.

Ullagaddi P.& Nagaraj, T. (2013). Investigation on geosynthetic reinforced two layered soil system. *Proceedings*, *7th international conference on case histories in geotechnical engineering,* Missouri University of Science and Technology, April 29- May 4.

Chen Q. & Farsakh, M.A. (2012). Structural contribution of geogrid reinforcement in pavement. In *Geo Congress: State of the Art and Practice in Geotechnical engineering* (1468-1475).

Archer S. & Wayne, M.H. (2012). Relevancy of Material Properties in Predicting the Performance of Geogrid-Stabilized Roadways. In *Geo Congress: State of the Art and Practice in Geotechnical Engineering*, 1320-1329.

Chen Q., Abu-Farsakh, M., Voyiadjis, G.Z., & Souci, G. (2012). Shakedown analysis of geogrid-reinforced granular base material. *Journal of Materials in Civil Engineering*, *25*(3), 337-346.

Giang N., Kuwano, J., Izawa, J., & Tachibana, S. (2010). Influence of unloading–reloading processes on the pullout resistance of geogrid. *Geosynthetic International*, *17*(4), 242-249.

Sarsam S., Al-Saeidy, A., & Falih, M. (2014). Assessing Pullout Resistance of Earth Reinforced Embankment Model. *Journal of Engineering Geology and Hydrogeology*, (JEGH), *2*(1), 9-14.

Abu-Farsakh, M., Ardah, A. & Voyiadjis, G. (2018). 3D Finite element analysis of the geosynthetic reinforced soil-integrated bridge system (GRS-IBS) under different loading conditions. *Transportation Geotechnics*, *15*, 70-83.

Ardah, A., Abu-Farsakh, M.Y. & Voyiadjis, G.Z. (2018). Numerical Evaluation of the Effect of Differential Settlement on the Performance of GRS-IBS. *Geosynthetic International*, 1-45.

American Society for Testing and Materials, ASTM- (2009). Road and Paving Material, Vehicle-Pavement System, *Annual Book of ASTM Standards*, Vol.04.03.

AASHTO, (2013). Standard Specification for Transportation Materials and Methods of Sampling and Testing, *American Association of State Highway and Transportation Officials*, 14th Edition, Part II, Washington, D.C.

Al Sandok A. (2018). Verification of layered theory for stabilized and reinforced subgrade model. *MSc. Thesis*, Department of Civil Engineering, University of Baghdad, Iraq.

Sarsam S. & Ibrahim, S. (2008). Contribution of liquid Asphalt in shear strength and rebound consolidation behavior of Gypseous soil. *Engineering and Technology*, *26*(4).

Sarsam S. & Barakhas, S. (2015). Assessing the Structural Properties of Asphalt Stabilized Subgrade Soil. *International Journal of Scientific Research in Knowledge*, (IJSRK), *3*(9), 0227-240.